Volume 26
Number 6
June 2024
Pages 959–1108

Environmental Science
Processes & Impacts

rsc.li/espi

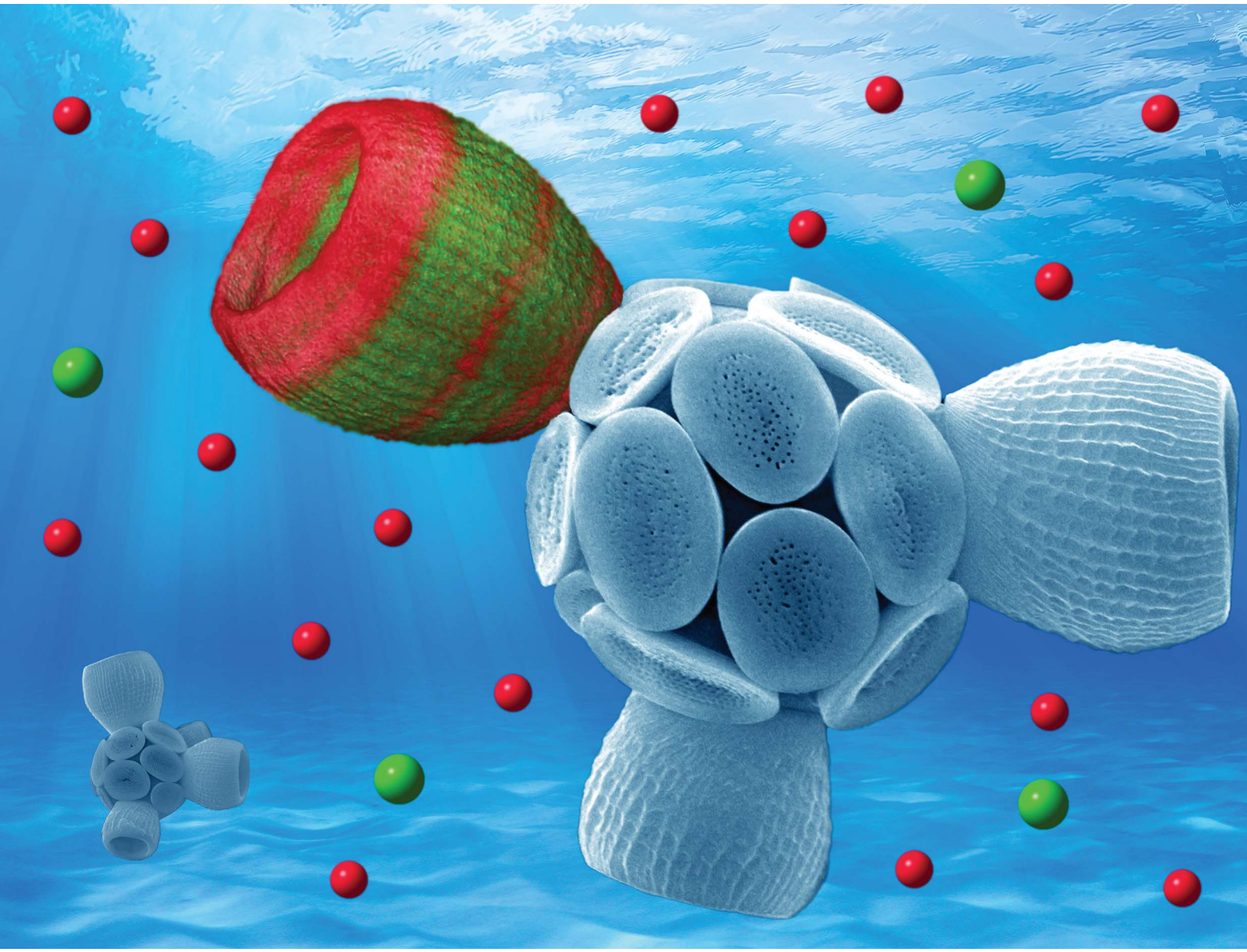

ISSN 2050-7887

ROYAL SOCIETY OF CHEMISTRY

PAPER

Jessica M. Walker, Gerald Langer *et al.*
An uneven distribution of strontium in the coccolithophore *Scyphosphaera apsteinii* revealed by nanoscale X-ray fluorescence tomography

Environmental Science Processes & Impacts

ROYAL SOCIETY OF CHEMISTRY

PAPER

View Article Online
View Journal | View Issue

Cite this: *Environ. Sci.: Processes Impacts*, 2024, **26**, 966

An uneven distribution of strontium in the coccolithophore *Scyphosphaera apsteinii* revealed by nanoscale X-ray fluorescence tomography†

Jessica M. Walker, *[a] Hallam J. M. Greene, [ab] Yousef Moazzam,[a] Paul D. Quinn,[a] Julia E. Parker [a] and Gerald Langer *[c]

Coccolithophores are biogeochemically and ecologically important phytoplankton that produce a composite calcium carbonate-based exoskeleton – the coccosphere – comprised of individual platelets, known as coccoliths. Coccoliths are stunning examples of biomineralization; their formation featuring exceptional control over both biomineral chemistry and shape. Understanding how coccoliths are formed requires information about minor element distribution and chemical environment. Here, the first high-resolution 3D synchrotron X-ray fluorescence (XRF) mapping of a coccolith is presented, showing that the lopadoliths of *Scyphosphaera apsteinii* display stripes of different Sr concentration. The presence of Sr stripes is unaffected by elevated Sr in the culture medium, macro-nutrient concentration, and light intensity, indicating that the observed stripiness is an expression of the fundamental coccolith formation process in this species. Current Sr fractionation models, by contrast, predict an even Sr distribution and will have to be modified to account for this stripiness. Additionally, nano-XANES analyses show that Sr resides in a Ca site in the calcite lattice in both high and low Sr stripes, confirming a central assumption of current Sr fractionation models.

Received 13th November 2023
Accepted 28th January 2024

DOI: 10.1039/d3em00509g

rsc.li/espi

Environmental significance

Coccolith composition is commonly used as a proxy for measuring the response of coccolithophores to environmental changes. The presence of coccoliths in the geological record means that proxy measurements can provide information about past climates. The Sr/Ca ratio of coccoliths is the most developed proxy for coccolithophore productivity, but understanding the mechanisms behind this proxy has been limited by the lack of nanoscale information about Sr distribution within individual coccoliths. Here, we use nanoscale XRF and XANES to map Sr and Ca within a coccolith of *Scyphosphaera apsteinii*, and show that the Sr/Ca ratio is not constant in this species, with Sr residing in the calcite lattice throughout. These observations help inform existing proxy models, and our understanding of coccolith biomineralization in general.

Introduction

Coccolithophores – unicellular calcifying marine microalgae – are important primary producers and are responsible for approximately half of global calcium carbonate production.[1,2] Coccolithophores produce calcite platelets, called coccoliths, that influence biogeochemical cycles through various mechanisms, not least through sinking and the eventual formation of calcareous sediments.[3] Nannofossil coccolith calcite is widely used in paleo-reconstructions of ocean ecosystem dynamics.[4] In particular, the Sr/Ca ratio of coccoliths has been used as a proxy for coccolith production and export, and remains the most widely applied geochemical proxy based on coccoliths.[5,6] Although the application of the Sr/Ca proxy has proved very successful, interpretation of the underlying mineral growth mechanisms can be difficult.[7,8] This difficulty stems mainly from the lack of relevant data used to constrain process-based biomineralization models. A key constraint required to inform such models is the distribution of Sr within a single coccolith. Coccolith Sr distribution is central to the development of biomineralization concepts that describe how these intricate structures are formed and how minor elements are incorporated. Minor element distribution can also be indicative of the crystallization mechanism employed in the formation of calcium carbonate biominerals. Extracellular calcifiers, such as bivalves, display a minor element banding pattern reflecting layered growth.[9] By contrast, coccolithophores (intracellular calcifiers) are thought to employ a simpler crystal growth

[a]*Diamond Light Source, Harwell Science and Innovation Campus, Didcot, Oxfordshire, OX11 0DE, UK. E-mail: jessica.walker@diamond.ac.uk*

[b]*Department of Chemistry, University of Sheffield, Dainton Building, Brook Hill, Sheffield S3 7HF, UK*

[c]*Institute of Environmental Science and Technology (ICTA), Universitat Autònoma de Barcelona (UAB), 08193 Bellaterra, Spain. E-mail: gerald.langer@cantab.net*

† Electronic supplementary information (ESI) available. See DOI: https://doi.org/10.1039/d3em00509g

mechanism, more akin to inorganic precipitation from an aqueous solution.[10] As such, any significant spatial variation in Sr/Ca within a coccolith would indicate refinement of our understanding of coccolith mineralization is required. One example of irregular Sr distribution in coccoliths in the fossil record is known (*Crepidolithus crassus*),[11] but this has not been reported for extant coccoliths.

One specific coccolithophore, *Scyphosphaera apsteinii*, is of particular interest in this context. This species has two coccolith types, flat muroliths and barrel-shaped lopadoliths (Fig. 1). It has recently been suggested that the lopadoliths of this species show an unexpected gradient of Sr from base to tip.[12] A Sr gradient does not directly support a layered growth mechanism but has important implications for biomineralization concepts because it is incompatible with steady state minor element fractionation models that predict an even distribution. Our current models for coccolithophores are such steady state models.[13,14] Modification of these models to account for an uneven minor element distribution would mark a major step in understanding biomineralization mechanisms. However, the suggestion that there is a Sr tip to base gradient in lopadoliths comes with a caveat, namely that the conclusion is based on Electron Dispersive X-ray spectroscopy (EDX) data, which has a limited resolution in relation to coccolith size, and relatively low accuracy when applied to the trace concentrations of Sr present.

Additionally, these models assume that Sr resides in coccolith calcite, an assumption that has only recently been tested for the placolith bearing species *Emiliania huxleyi*.[15] Although it was shown that Sr resides in *E. huxleyi* calcite, it is unknown whether this holds for *S. apsteinii*. There are several important differences between these two species. Firstly, they are phylogenetically distant and might have different minor element fractionation mechanisms.[16] Secondly, *S. apsteinii* has an atypically high Sr/Ca ratio (and Sr partitioning coefficient, D_{Sr}) compared to placolith bearing species such as *E. huxleyi*, *Coccolithus braarudii*, and *Helicosphaera carteri*.[7,12,17,18] This high Sr/Ca ratio is also observed in *C. crassus*, the fossil example of uneven Sr distribution.[11] Thirdly, *S. apsteinii* is a dimorphic species featuring disc-shaped muroliths and barrel-shaped lopadoliths that grow from a murolith base extending the wall to form the barrel,[19,20] whereas *E. huxleyi* and other placolith bearing species are limited to one coccolith morphology in their heterococcolith stage. Finally, *S. apsteinii* lopadoliths have an inner layer of foliate crystals (R units) that do not nucleate on the base plate but have various nucleation points, presumably on the organic material that is located between the individual crystals.[19,20] These specific features of *S. apsteinii* pose the question whether Sr might reside in the organic material between foliate R unit crystals as opposed to the calcite lattice of

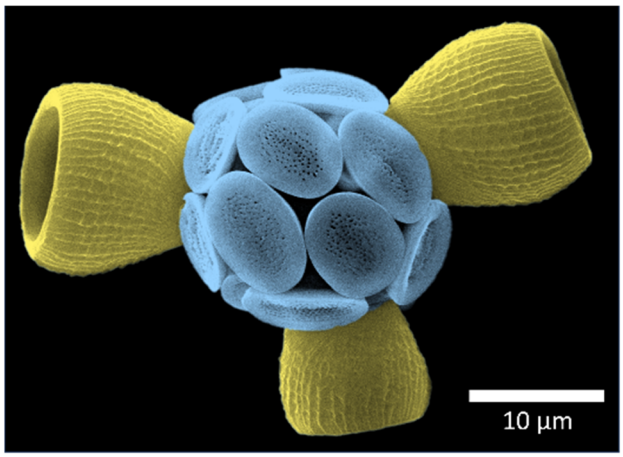

Fig. 1 False colour scanning electron micrograph of a *Scyphosphaera apsteinii* coccosphere, showing the flat muroliths (blue) and three barrel-shaped lopadoliths (yellow).

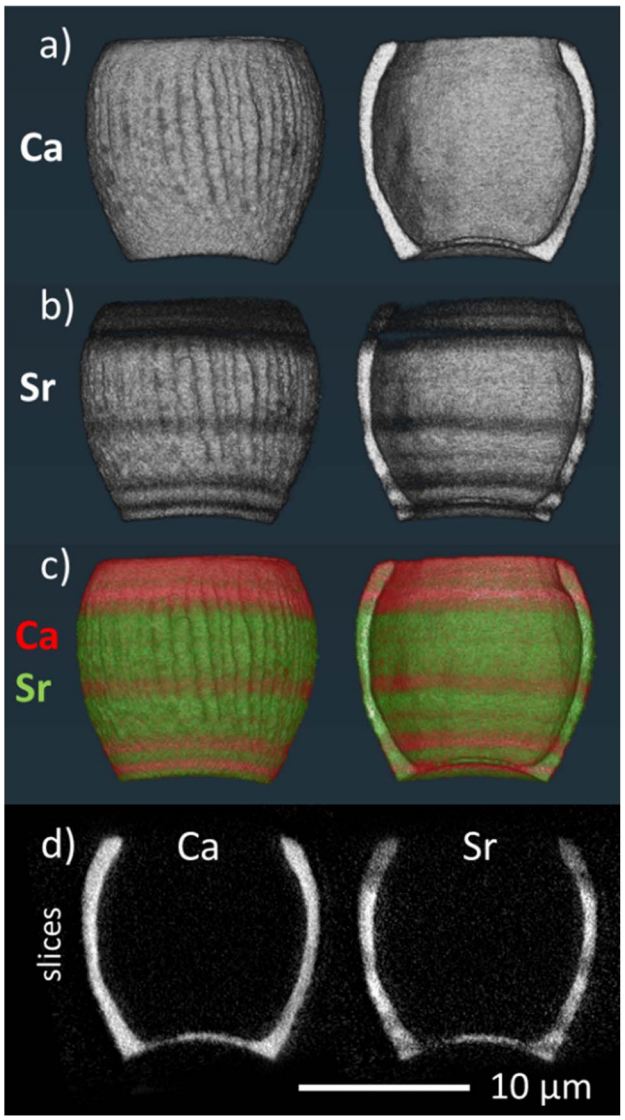

Fig. 2 3D volume renderings of the reconstructed 3D XRF data for (a) calcium and (b) strontium signals individually and (c) combined (calcium signal in red, strontium signal in green), showing both the full image of the lopadolith and a cut through along the growth direction. The corresponding reconstruction slices are also shown (d). For additional views and a blue-yellow rendering, refer to Fig. S3 and S4.† An example XRF spectrum from a single pixel is shown in Fig. S5.†

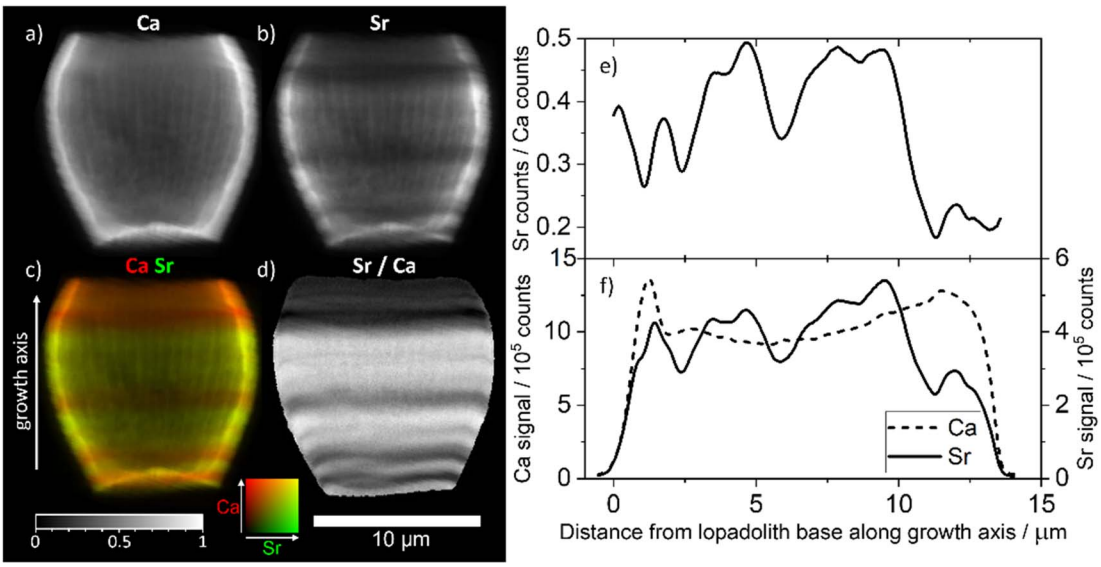

Fig. 3 XRF elemental maps of the lopadolith scanned at a 60 nm resolution with a 0.75 s count time. (a) Calcium counts; (b) strontium counts; (c) composite image of a and b with the Ca signal in red and Sr signal in green, with the growth axis labelled; (d) result of dividing the Sr counts by the Ca counts in each pixel. The 10 µm scale bar applies to all maps. XRF maps are individually normalised from 0–1, the maximum counts per pixel (displayed as white) are given in Table S1.† (e) The value of the Sr counts divided by the Ca counts, and (f) the sum of Ca and Sr counts, as a function of distance along the growth axis. XRF counts are windowed and therefore not corrected for air path, self absorption or energy differences. Example raw XRF spectrum from a single pixel is available in Fig. S6.†

these crystals. Inorganic precipitation experiments have shown that a D_{Sr} as high as 0.38 can be achieved without forming strontianite phases.[21] Hence inorganic fractionation could explain the D_{Sr} of placolith bearing species, but *S. apsteinii* displays D_{Sr} values of up to 3.7, an order of magnitude above the maximum value that has been achieved in inorganic precipitation experiments.[12] The formation of other Sr-rich mineral phases such as strontianite or aragonite is unlikely as previous work has detected only calcite in the powder X-ray diffraction patterns of *S. apsteinii* coccoliths.[17] Therefore, one explanation for this unusually high Sr/Ca ratio could be a substantial fractionation of Sr into organic material.

In this work, we have examined the distribution of Sr within a single lopadolith, using high-resolution synchrotron X-ray fluorescence (XRF) mapping in three dimensions, alongside 2D XRF imaging to fully characterise the elemental composition of the lopadoliths. In addition, we have determined the environment of Sr in these high D_{Sr} coccoliths, using XANES Sr K-edge mapping. These experiments provide vital information for biomineralization models, and further insight into coccolithogenesis in *S. apsteinii*.

Results and discussion

A stripy Sr distribution

To investigate how the Sr/Ca ratio varies across an individual lopadolith, we used X-ray fluorescence (XRF) at the hard X-ray nanoprobe, beamline I14 at Diamond Light Source. Using a nominal 50 nm beam size,[22] it is possible to measure elemental composition at high resolution. Initial 2D XRF mapping of a single lopadolith showed that there were several 'stripes' where the Sr concentration varied, whereas the Ca signal remained consistent, taking into account the structure of the lopadolith (Fig. 3).

However, the shape of a lopadolith is by its nature different in three dimensions, having a barrel-like shape that is open on the distal side. To fully understand its structure, therefore, tomographic imaging is required. Using XRF tomography at the hard X-ray nanoprobe (I14), we have imaged the elemental composition of an individual lopadolith of *S. apsteinii* in three-dimensions. Individual 2D XRF projections were taken at a series of angles and the Ca and Sr signals were reconstructed and the volumes combined. Images from the merged volume and slices from the elemental reconstructions are shown in Fig. 2, with further views in Fig. S3 and ESI Video 1.†

These element specific volumes show a number of features, with sufficient resolution to visualise the vertical ridges commonly seen by scanning electron microscopy (SEM) of lopadoliths (Fig. 1). There are Sr stripes throughout the 3D structure, showing that fractionation of Sr into the coccolith varies within a single lopadolith growth period. These stripes are unbroken rings around the growth axis of the coccolith (*i.e.* variations occur in the growth direction). This is a surprising result because the current model of coccolith formation predicts an even distribution of Sr, and only one example of experimental evidence has suggested any kind of concentration gradient.[12] Whilst coccolith crystal growth is assumed to resemble inorganic precipitation from an aqueous solution,[23] recent high-resolution studies on both cellular and coccolith architecture have added important modifications to this picture.[24,25] However, the latter studies also provide new evidence supporting the hypothesis that coccolith crystal

growth is controlled by steady state ion fluxes in the coccolith vesicle. This steady state assumption is a central component of Sr fractionation models which consequently predict an even distribution of Sr in coccoliths.[13,14] Measurements from a number of techniques for analysing compositional distribution (XRF, secondary ion mass spectrometry (SIMS), and nanoSIMS) on *Coccolithus braarudii* and *Watznaueria* suggest an even Sr distribution, supporting the model assumption, with only the fossil *C. crassus* showing any variation.[11,26–28] By contrast in *S. apsteinii*, the XRF data presented here present a challenge to this assumption, showing a difference in Sr/Ca ratios within a single coccolith. As shown in Fig. 2, the XRF data clarify that rather than a Sr/Ca gradient,[12] there are stripes of different Sr/Ca ratios throughout the lopadolith. This evidence is important because the mechanisms underlying these two patterns of Sr distribution might be fundamentally different. A banding pattern is reminiscent of the situation in extracellular calcifiers where it corresponds to layered growth.[9] Whilst the Sr banding patterns shown here could point to layered growth in *S. apsteinii*, more work on the growth process and structure of the lopadolith is needed to definitively answer this question. If layered growth was confirmed, this would have far-reaching consequences for our understanding of calcification in general. However, a crucial unanswered question in this context is the nano-structure of coccolith crystals in *S. apsteinii*. Despite the availability of relevant data in the literature it is still unclear whether coccolith crystals feature an "extracellular-like" nano-structure, a central indicator of layered growth.[10] If coccolith crystals did not display an "extracellular-like" nano-structure the stripiness shown here would likely have an origin other than layered growth. Another consideration is the evolution of calcification mechanisms. Since layered growth is present in a range of extracellular calcifiers across the phylogenetic spectrum, *e.g.* molluscs and foraminifera, it seems to be a highly conserved mechanism, deep-rooted in evolutionary history.[29] Therefore, we would expect that, if coccolithophores also feature layered growth, they should do so as a group. Judging from Sr fractionation alone, however, there is reason to believe that *S. apsteinii* is different from other species, particularly placolith bearing ones. As mentioned above, *C. braarudii* seems to display an even Sr distribution. A second difference is the partitioning coefficient which is *ca.* 0.3 in placolith bearing species but an order of magnitude higher in *S. apsteinii*.[12,17] A high Sr partitioning coefficient seems to be a feature of some murolith forming species such as *S. apsteinii*, *Pontosphaera*, and the Jurassic *C. crassus*.[11,12,17] It is interesting to note that *C. crassus* also features an uneven Sr distribution, although not a stripy pattern as in *S. apsteinii* as shown in this study.[11] It is impossible to know whether the mechanisms underpinning the high Sr partitioning coefficient and uneven Sr distribution in the Jurassic *C. crassus* and the extant *S. apsteinii* are similar. It is, however, intriguing to speculate that there is some kind of connection between a high Sr partitioning coefficient and an uneven Sr distribution. It will be highly useful to have information about the Sr distribution in other placolith bearing species, phylogenetically both close and distant to *S. apsteinii*, which would answer the question whether a mechanistic connection between bulk Sr partitioning and distribution is likely.

Assuming for argument's sake that *S. apsteinii* is special among coccolithophores and that coccolithophores do not feature layered growth of coccoliths, how could we interpret the Sr stripiness (in distinction to "banding" indicating layered growth)? Before we discuss the interpretation of these observations, it is necessary to examine the scale of the Sr variations to show that they are not merely noise, and, in fact, tally well with banding variations in extracellular calcifiers.

The scale of stripes

To examine the scale of this variation we used the 3D tomogram to pick an angle where the growth axis of the lopadolith was at 90° from the beam (*i.e.* optimally aligned), and from this projection (Fig. 3a–d) we were able to take a cross section through the stripes without any interference from a different feature on the back of the barrel. Working at this angle, we plotted the sum of the Sr and Ca counts as a function of the distance along the growth axis (Fig. 3c, arrow, *x* axis). This plot is shown in Fig. 3f. The value of the Sr counts/Ca counts at each distance is given in Fig. 3e. An example XRF spectrum from a single pixel of one projection is shown in Fig. S5.†

The measured Sr and Ca XRF counts have not been corrected for factors such as air path to the detector or cross-section differences due to the energy used (18 keV). The structure is hollow, with small slowly varying thickness variations of ±10% as can be seen from the slices and Ca profile in Fig. 3a and f. Self-absorption of the Ca signal is therefore considered as broadly consistent effect. The ratio of Sr counts/Ca counts between regions can therefore be compared in a relative sense within each lopadolith (Fig. 3e) but the ratio within a specific region is not a quantitative measurement. A differential phase contrast (DPC) image of the same coccolith measured simultaneously shows how the density varies, which is largely reflective of the Ca signal (Fig. S1†). The DPC image also confirms the increase in Ca signal at the rim is due to an increase in thickness.

Using these graphs (Fig. 3e and f), and the approximation that the ratio of Sr counts/Ca counts is proportional to the molar Sr/Ca ratio, we can see that the increase in the relative Sr/Ca ratio between the rim and the highest Sr 'stripe' is almost 2.5 times the value of the rim. The central stripe of low Sr has a Sr/Ca count ratio of approx. 0.7 times less than that of the highest Sr/Ca ratio region. In the bivalve *Arctica islandica*, Sr/Ca varies by a factor of 1.3–1.6 along a shell transect.[30] Hence the Sr variation due to stripes in *S. apsteinii* is similar in scale to the one due to banding in *A. islandica*.

Variable stripe number and width

As the timescales involved in XRF tomography are long, only one individual could be imaged in 3D, therefore we mapped several further lopadoliths in 2D using XRF (Fig. 4). Having established using the above tomogram that the observed stripes in 2D are continuous rings around the growth axis, we can safely

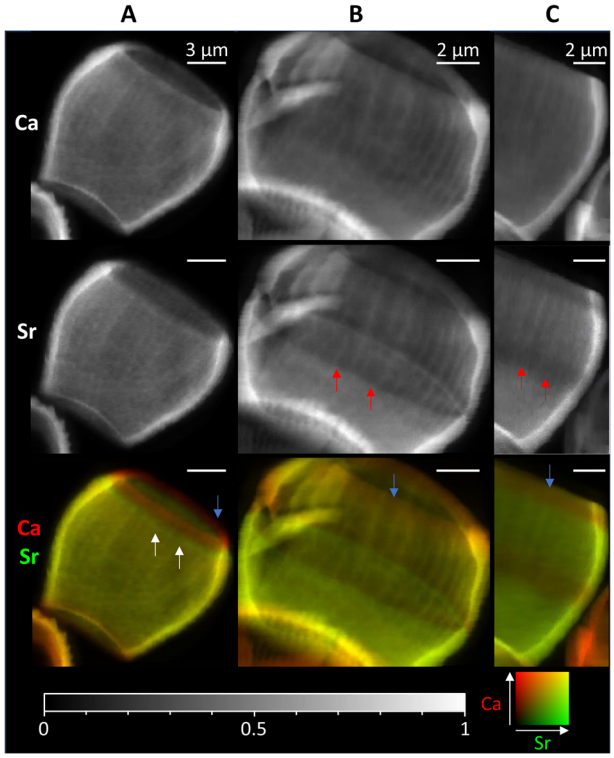

Fig. 4 2D XRF images of lopadoliths from different cultures, showing the Ca and Sr signals individually and combined. (Ca – red, Sr – green). White arrows show rings of high Sr and red arrows rings of low Sr regions. Blue arrows show the low Sr rim at the top. These were grown at (A) Diamond Light Source and (B) and (C) Marine Biological Association, Plymouth. Count times and step sizes varied between 0.15 s at 50 nm step (C), 0.5 s at 100 nm step (A) and 1 s at 50 nm step (B) XRF maps are individually normalised from 0–1, the maximum counts per pixel (displayed as white) are given in Table S1.† An additional coccolith image and alternative colour scheme images for the bottom row are given in Fig. S9.†

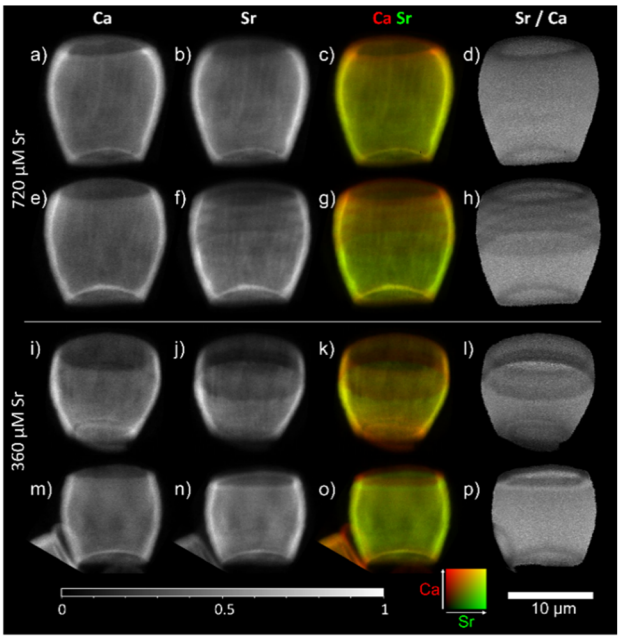

Fig. 5 2D XRF images of lopadoliths from cultures grown in media at higher than ambient Sr concentrations: 720 µM (top, a–h) and 360 µM Sr (bottom, i–p) rows represent different lopadoliths and contain a map of Ca counts, a map of Sr counts, a composite image with Ca signal in red and Sr signal in green, and a map showing the result of dividing the Sr counts by the Ca counts per pixel. Maps were collected at a count time of 0.05 s per pixel. The 10 µm scale bar applies to all images. XRF maps are individually normalised from 0–1, the maximum counts per pixel (displayed as white) are given in Table S1.† Alternative colour scheme images for (c, g, k, and o) can be found in Fig. S10.†

assume that a similar structure observed in other 2D XRF maps will follow the same pattern in 3D.

These 2D maps revealed that stripiness of some kind is present across individuals, but that the pattern varies in width and/or number of stripes, and their position. These coccoliths represent specimens from cultures grown in two separate locations from different starter cultures, demonstrating that Sr stripiness is not unique to a specific culture or culturing method.

Some features are consistent, a band of higher concentration Sr (white arrows) or a band of lower concentration Sr (red arrows) is generally seen, although these vary in size and position. However, in every lopadolith there is a low Sr rim (blue arrows, bottom row) at the top of the barrel shape which is found in each example measured. This suggests this is a key requirement for the lopadolith growth, that is likely directed as part of the biomineralization process. Previous work[12] has reported that the Sr concentration is less at the top of the coccolith which we confirm here, but the XRF evidence shows this is limited to a small rim only. Potential causes of this variation between specimens is discussed in a later section.

Impact of [Sr] in the culture media

We have also considered whether varying Sr concentration in the growing media may impact the presence of the stripes. Previous work using EDX[12] did not determine any significant difference in Sr/Ca ratio between the base and tip of the lopadolith grown at higher Sr concentrations, suggesting the growth media Sr concentration may have an impact on the Sr distribution. To explore whether the growth media Sr had an impact on the observed stripiness, we examined cultures grown in two higher [Sr] media, 360 and 720 µM. As shown in Fig. 5, stripes were observed in all cases, with variation in placement as observed with those grown at ambient [Sr], therefore the Sr concentration of the media appears not to affect the occurrence of stripes. Again, the rim showed a lower Sr/Ca ratio, a feature that was conserved across all samples imaged (as shown in by blue arrows in Fig. 4), thus the low Sr rim is unaffected by change in [Sr] in the media.

Potential causes of Sr stripes in *S. apsteinii*

Before we disregard layered growth, we will discuss the possibility that the foliate crystals (R units)[19] of the inner lopadolith layer play the role of nanoscale crystallites (as revealed by AFM) in extracellular calcifiers. To simplify we can say that the latter produce these crystallites by depositing ACC in an organic hydro-gel and transforming it to a crystalline polymorph such

as calcite.[9] The crystallites are embedded in an organic framework. In *S. apsteinii*, lopadolith walls are made up of an outer layer and inner foliate crystals.[19,20] The 3D XRF imaging suggests that the Sr/Ca count ratio variation is consistent throughout the wall thickness, which means that the outer and inner layers are formed concurrently, although it may not be possible to distinguish a very thin layer (less than 150 nm) at this imaging resolution. Previous work using TEM and SEM[20] imaged the interior wall structure, which showed the inner foliate crystals are relatively thin, and suggested that there are a number of nucleation points as the lopadolith walls form. This design would allow for the crystal composition to vary in response to local Sr concentration changes over a shorter timescale as the lopadolith forms, rather than in other coccolithophores which grow comparatively larger single crystals, usually beginning from initial rhombohedral proto-coccolith ring crystals. In addition, TEM studies showed the presence of an organic material in between the crystals, which is more similar to a layered growth system, and would certainly allow for manipulation of the Sr/Ca ratio between individual crystals.[20] Therefore, there are parallels between the foliate crystals in *S. apsteinii* and the nanoscale crystallites in extracellular calcifiers, but there is also a difference: crystallites of extracellular calcifiers have a rounded surface and never display any faceted crystal surfaces.[29] The foliate crystals of *S. apsteinii*, by contrast, do display faceted crystal surfaces.[20] Another morphological feature of layered growth not present in *S. apsteinii* is an "organic banding" in parallel with the elemental (*e.g.* Sr) banding.[29] Therefore, they might be produced by a fundamentally different mechanism, *i.e.* not layered growth. The nature of this different mechanism remains an open question. Possibilities include kinetic effects during crystal growth, the use of a different Ca^{2+} transport pathway, and the use of different coccolith-associated polysaccharides (CAP) with different Sr fractionation behaviour. It is instructive to keep in mind that the Sr stripes vary between specimens in number, size, and position (see figures above). What causes a low or high Sr stripe to occur is unknown, but the variability of pattern does point towards a change in ion transport or availability during the formation of a single lopadolith. As the stripes are perpendicular to the growth direction, variation in Sr/Ca ratio occurs as a function of time – *i.e.* calcite formed at the same time has the same Sr/Ca ratio. As Sr/Ca ratio is known to be influenced by growth rate (in both biomineral and inorganic systems)[31,32] this could present an explanation. However, causes of the variation in growth rate during the production of an individual lopadolith are not clear, as external factors such as temperature and light/dark cycling are kept constant and/or are longer than the time frame of a single coccolith growth period.[5,33] It should be noted that potential crystal growth rate effects on variable Sr fractionation (stripe formation) have no necessary link with the application of coccolith Sr/Ca as productivity proxy. Briefly, Sr/Ca is not a cell division- or calcification rate proxy, and the correlation of Sr/Ca and productivity in field data is still poorly understood.[7,13]

The direction of crystal growth has also been postulated to be a contributing factor to Sr^{2+} incorporation, however, there are contradicting reports regarding whether the R or V unit growth direction most favours Sr^{2+} incorporation, and this alone is unlikely to lead to the striped pattern observed.[11,17] In the specimen imaged in 3D, the base of the coccolith also contains variations, which match the height of the stripes in the side walls (Fig. S3†). This would suggest these regions are growing at the same time, and, as the base region has a different crystal organisation, would be evidence against specific crystal growth directions being the main contributing factor.

A further mechanism to consider is variations in ion transport, which lead to changes in the intracellular environment during the growth period. Virtually all eukaryotic cells use a suite of ion-conducting proteins including channels and ATP-driven transporters.[34,35] It can safely be assumed that all Ca transporting proteins will transport Sr too, but the Sr fractionation factor will vary between different proteins.[8,33] These Sr fractionation factors are unknown for coccolithophores. It has been emphasized recently that *C. braarudii* alone possesses three different Ca channels of unknown Sr fractionation.[8] The overall Sr fractionation into coccoliths then depends on the relative ion fluxes of these transport proteins. Slight changes in, for example, plasma membrane voltages can change the relative fluxes of voltage-gated Ca channels, and could solely be responsible for Sr stripes in *S. apsteinii*. Further understanding of coccolithogenesis and cellular processes in coccolithophores is required to answer these questions. However, the low Sr rim (Fig. 4, blue arrows) is consistent in every specimen, which suggests that, regardless of the cause of intermediary stripes, there might be an additional stripe-generating mechanism that is tightly linked to the finalization of lopadolith formation. This suggests that the low Sr rim is coupled to some essential process at the end of calcification, whereas the other stripes are not necessarily related to specific morphological features, and as shown in Fig. 5, unrelated to the media [Sr]. This essential process could be the- still enigmatic- "stop signal" of coccolith growth.[36] It could also point to a slowing down of crystal growth rate, which is positively correlated to Sr/Ca.[37,38] It is also possible that a special type of CAP is used to terminate coccolith crystal growth. This "termination-CAP" could introduce a different Sr fractionation in one of three ways as discussed by Meyer *et al.* (2020).[12] One option is that Sr resides partly in CAP, and that different CAPs have different Sr partitioning coefficients. In order to explore this option, we conducted X-ray absorption Near Edge Spectroscopy (XANES) mapping.

Sr resides in calcite

To answer the question whether the uneven Sr distribution is caused by fractionation of Sr into an organic phase or another mineral phase, we used X-ray Absorption Near Edge Spectroscopy (XANES) mapping to investigate what Sr environments were present in the lopadolith and whether this varied with the concentration of Sr. Previous work has shown that Sr K-edge XANES is sensitive to Sr in a specific polymorph of calcium carbonate,[39] and to the coordination environment of the Sr within calcite itself.[40] Using the optimum projection angle as described above, we mapped a transect across the stripes (Fig. 6A, red box) at 152 energies, creating a XANES spectra at each pixel.

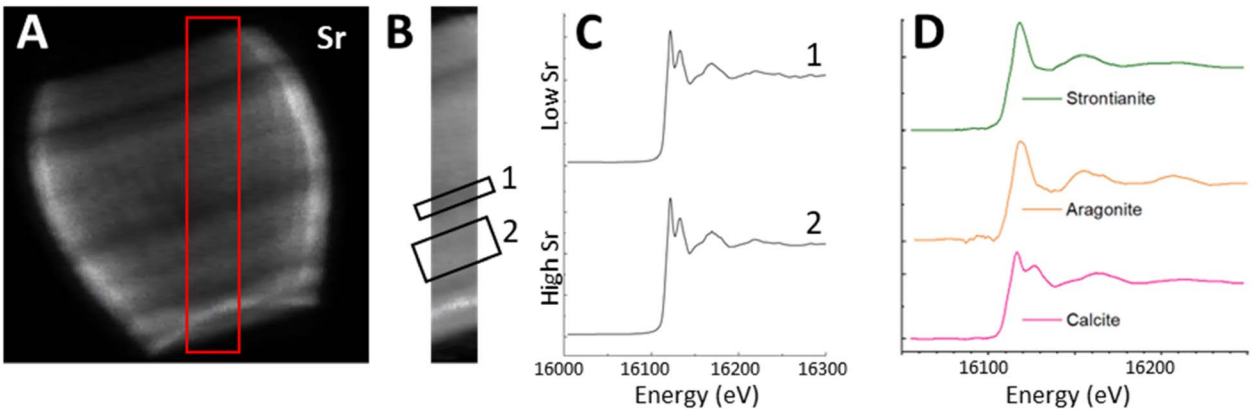

Fig. 6 Using the Sr XRF map (A), a transect (red box in (A) was selected for mapping over the Sr K-edge. (B) shows the transect in isolation and the location of region 1 (low Sr) and 2 (high Sr). The Sr K-edge XANES spectra from all pixels in each region were summed to give graphs shown in (C). XANES spectra of standards from bulk XANES measured at the beamline are shown in (D).

Fig. 6B shows the Sr XRF map of the transect at a beam energy of 16.2 keV (*i.e.* above the Sr K-edge). We selected two regions of interest (ROIs), one in the high Sr region, and one in the low Sr region, and summed across all the pixels in each ROI to produce an average XANES spectra for each region (Fig. 6C). Both regions showed a XANES spectra similar to that of Sr in calcite, with a characteristic near-edge second peak (Fig. 6D) suggesting the Sr is in a calcium site within the calcite lattice. This confirms that despite the spatial variation in Sr concentration, and the high Sr/Ca ratio observed in this species, the Sr environment appears to consistently resemble Sr within the mineral calcite phase in a Ca site,[40] as opposed to containment within organic phases or other mineral phases.

While this result rules out one of the possible ways in which CAP could alter Sr fractionation,[12] there is a more profound significance here. The fact that Sr resides in calcite despite the variation in Sr/Ca ratio, and the overall high Sr content of *S. apsteinii*,[12,17] confirms a central assumption of Sr fractionation models. These conceptual models assume that an important part of the overall fractionation process is the incorporation of Sr into the calcite lattice in a calcium site.[13,14] The first process-based minor element fractionation models that were developed for marine calcifiers explained the fractionation solely in terms of inorganic precipitation from seawater; only later were biological fractionation steps added.[8,41] These biological fractionation steps have been recognised as essential in explanations of Sr fractionation into coccoliths.[13,18] The localization of Sr in a calcium site of the calcite lattice (Fig. 6) implies that Sr fractionation into lopadoliths of *S. apsteinii* requires a coccolith vesicle Sr/Ca ratio that is substantially higher than the one of placolith bearing species such as *E. huxleyi* and *C. braarudii*.[12,13,17,21] Further studies investigating the differences in Sr fractionation between *S. apsteinii* and placolith bearing species are clearly warranted.

Conclusions

In this work we have shown *via* XRF imaging and tomography that *S. apsteinii* lopadoliths have an uneven Sr distribution, displaying stripes of different Sr concentration. This is not explained by standard models for Sr fractionation into coccoliths, and demonstrates the need for a deeper understanding of coccolithogenesis. Moreover, it seems likely that an uneven Sr distribution is a specific feature of the Pontosphaeraceae, maybe even of *S. apsteinii* alone amongst extant species. Therefore, other species should be analysed to determine whether family-specific, or even species-specific models need to be developed. Additionally, we show that Sr substitutes for Ca in the calcite lattice, in both higher and lower concentration Sr stripes. This means that intra-lopadolith Sr variations are not caused by Sr incorporation into organic material.

Data availability

Methods are found in the ESI.† Data is available on request.

Author contributions

JW and GL conceived the study, performed the experimental work, and lead the manuscript writing and editing. YM and PQ worked on the data analysis methods, software, and reviewed and edited the manuscript draft. JP provided supervision and experimental assistance, and reviewed and edited the manuscript draft. HG performed the experimental work, contributed to figure production and the original manuscript drafting, and reviewed and edited the manuscript.

Conflicts of interest

There are no conflicts to declare.

Acknowledgements

We acknowledge Diamond Light Source for time on Beamline I14 under proposal mg31325. Cultures were grown using facilities provided by the Research Complex at Harwell (RCaH). SEM images were generated using the electron microscopy facilities at the RCaH. Funding for this study and for a studentship (HG)

was provided by Diamond Light Source. We acknowledge Diamond Light Source for time on the laboratory diffractometer in their Optics laboratories. We thank Timothy Poon for his computing assistance, and Mark Hooper and David Mahoney for their technical and engineering help. GL acknowledges funding from the Spanish Ministry of Universities through a Maria Zambrano grant and the Generalitat de Catalunya (MERS, 2021 SGR 00640). This work contributes to ICTA-UAB "María de Maeztu" Programme for Units of Excellence of the Spanish Ministry of Science and Innovation (CEX2019-000940-M). We also thank Ian Probert and Martin Gachenot for helping with the cultures.

References

1 W. M. Balch, The Ecology, Biogeochemistry, and Optical Properties of Coccolithophores, *Annu. Rev. Mar. Sci.*, 2018, **3**, 71–98.
2 C. J. Daniels, A. Poulton, W. M. Balch, E. Marañón, T. Adey, B. C. Bowler, P. Cermeño, A. Charalampopoulou, D. W. Crawford, D. Drapeau, Y. Feng, A. Fernández, E. Fernández, G. M. Fragoso, N. González, L. M. Graziano, R. Heslop, P. M. Holligan, J. Hopkins, M. Huete-Ortega, D. A. Hutchins, P. J. Lam, S. M. Lipsen, D. C. López-Sandoval, S. Loucaides, A. Marchetti, K. M. J. Mayers, A. P. Rees, C. Sobrino, E. Tynan and T. Tyrrell, A global compilation of coccolithophore calcification rates, *Earth Syst. Sci. Data*, 2018, **10**, 1859–1876.
3 *Coccolith Contribution to South Atlantic Carbonate Sedimentation*, ed. K. H. Baumann, B. Bockel and M. Frenz, Springer Berlin, Heidelberg, 2004.
4 J. A. Flores, F. J. Sierro, G. Frances, A. Vazquez and I. Zamarreno, The last 100,000 years in the western Mediterranean: sea surface water and frontal dynamics as revealed by coccolithophores, *Mar. Micropaleontol.*, 1997, **29**, 351–366.
5 H. M. Stoll, N. Shimizu, A. Arevalos, N. Matell, A. Bansiak and S. Zeren, Insights on coccolith chemistry from a new ion probe method for analysis of individually picked coccoliths, *Geochem., Geophys., Geosyst.*, 2007, **8**, Q06020.
6 C. Cavaleiro, A. H. L. Voelker, H. Stoll, K. H. Baumann, D. K. Kulhanek, B. D. A. Naafs, R. Stein, J. Grutzner, C. Ventura and M. Kucera, Insolation forcing of coccolithophore productivity in the North Atlantic during the Middle Pleistocene, *Quat. Sci. Rev.*, 2018, **191**, 318–336.
7 H. M. Stoll and P. Ziveri, in *Coccolithophores*, ed. H. R. Thierstein and J. R. Young, Springer, Berlin, Heidelberg, 2004.
8 G. Nehrke and G. Langer, Proxy Archives Based on Marine Calcifying Organisms and the Role of Process-Based Biomineralization Concepts, *Minerals*, 2023, **13**, 561.
9 J.-P. Cuif, Y. Dauphin, G. Nehrke, J. Nouet and J. Perez-Huerta, Layered Growth and Crystallization in Calcareous Biominerals: Impact of Structural and Chemical Evidence on Two Major Concepts in Invertebrate Biomineralization Studies, *Minerals*, 2012, **2**, 11–39.
10 J. M. Walker and G. Langer, Coccolith crystals: Pure calcite or organic-mineral composite structures?, *Acta Biomater.*, 2021, **125**, 83–89.
11 B. Sucheras-Marx, F. Giraud, A. Siminovici, R. Tucoulou and I. Daniel, Evidence of high Sr/Ca in a Middle Jurassic murolith coccolith species, *Peer community palaeontol*, 2021, **1**, e25.
12 E. M. Meyer, G. Langer, C. Brownlee, G. L. Wheeler and A. R. Taylor, Sr in coccoliths of *Scyphosphaera apsteinii:* partitioning behavior and role in coccolith morphogenesis, *Geochim. Cosmochim. Acta*, 2020, **285**, 41–54.
13 G. Langer, N. Gussone, G. Nehrke, U. Riebesell, A. Eisenhauer, H. Kuhnert, B. Rost, S. Trimborn and S. Thoms, Coccolith strontium to calcium ratios in *Emiliania huxleyi*: The dependence on seawater strontium and calcium concentrations, *Limnol. Oceanogr.*, 2006, **51**, 310–320.
14 L. M. Mejia, A. Paytan, A. Eisenhower, F. Bohm, A. Kolevica, C. Bolton, A. Mendez-Vincente, L. Abrevaya, K. Isensee and H. Stoll, Controls over d44/40Ca and Sr/Ca variations in coccoliths: New perspectives from laboratory cultures and cellular models, *Earth Planet. Sci. Lett.*, 2018, **481**, 48–60.
15 A. Gal, S. Sviben, R. Wirth, A. Schreiber, B. Lassalle-Kaiser, D. Faivre and A. Scheffel, Trace-Element Incorporation into Intracellular Pools Uncovers Calcium-Pathways in a Coccolithophore, *Adv. Sci.*, 2017, **4**, 1700088.
16 J. Henderiks, D. Sturm, L. Supraha and G. Langer, Evolutionary Rates in the Haptophyta: Exploring Molecular and Phenotypic Diversity, *J. Mar. Sci. Eng.*, 2022, **10**(6), 798.
17 M. Hermoso, B. Lefeuvre, F. Minoletti and M. D. Rafelis, Extreme strontium concentrations reveal specific biomineralization pathways in certain coccolithophores with implications for the Sr/Ca paleoproductivity proxy, *PLoS One*, 2017, **12**, e0185655.
18 H. M. Stoll, Y. Rosenthal and P. Falkowski, Climate proxies from Sr/Ca of coccolith calcite: calibrations from continuous culture of *Emiliania huxleyi*, *Geochim. Cosmochim. Acta*, 2002, **66**, 927–936.
19 J. Young, *Scyphosphaera porosa* Kamptner 1967, Rediscovered in the plankton, *J. Nannoplankton Res.*, 2008, **30**, 35–38.
20 B. Drescher, R. M. Dillaman and A. R. Taylor, Coccolithogenesis In *Scyphosphaera apsteinii* (Prymnesiophyceae), *J. Phycol.*, 2012, **48**, 1343–1361.
21 I. R. Gabitov and E. B. Watson, Partitioning of strontium between calcite and fluid, *Geochem., Geophys., Geosyst.*, 2006, **7**, Q11004.
22 P. D. Quinn, L. Alianelli, M. Gomez-Gonzalez, D. Mahoney, F. Cacho-Nerin, A. Peach and J. E. Parker, The Hard X-ray Nanoprobe beamline at Diamond Light Source, *J. Synchrotron Radiat.*, 2021, **28**, 1006–1013.
23 J. R. Young, S. A. Dean, P. R. Bown and S. Mann, Coccolith Ultrastructure and Biomineralisation, *J. Struct. Biol.*, 1999, **126**, 195–215.
24 Y. Kadan, F. Tollervey, N. Varsano, J. Mahamid and A. Gal, Intracellular nanoscale architecture as a master regulator

of calcium carbonate crystallization in marine microalgae, *Proc. Natl. Acad. Sci. U. S. A.*, 2021, **118**, e2025670118.

25 E. M. Avrahami, L. Houben, L. Aram and A. Gal, Complex morphologies of biogenic crystals emerge from anisotropic growth of symmetry-related facets, *Science*, 2022, **376**, 312–316.

26 C. R. M. Grovenor, K. E. Smart, M. R. Kilburn, B. Shore, J. R. Dilworth, B. Martin, C. Hawes and R. E. M. Rickaby, Specimen preparation for NanoSIMS analysis of biological materials, *Appl. Surf. Sci.*, 2006, **252**, 6917–6924.

27 K. Prentice, T. Dunkley-Jones, J. Lees, J. Young, P. Bown, G. Langer and S. Fearn, Trace metal (Mg/Ca and Sr/Ca) analyses of single coccoliths by Secondary Ion Mass Spectrometry, *Geochim. Cosmochim. Acta*, 2014, **146**, 90–106.

28 B. Sucheras-Marx, F. Giraud, A. Simionovici, I. Daniel and R. Tucoulou, Perspectives on heterococcolith geochemical proxies based on high-resolution X-ray fluorescence mapping, *Geobiology*, 2016, **14**, 390–403.

29 J.-P. Cuif, Y. Dauphin and J. E. Sourauf, *Biominerals and Fossils Through Time*, Cambridge University Press, 2011.

30 L. C. Foster, N. Allison, A. A. Finch and C. Andersson, Strontium distribution in the shell of the aragonite bivalve Arctica islandica, *Geochem., Geophys., Geosyst.*, 2009, **10**, Q03003.

31 M. Inoue, A. Suzuki, M. Nohara, K. Hibino and H. Kawahata, Empirical assessment of coral Sr/Ca and Mg/Ca ratios as climate provies using colonies grown at different temperatures, *Geophys. Res. Lett.*, 2007, **34**, L12611.

32 J. Tang, A. Niedermayr, S. J. Kohler, F. Bohm, B. Kisakurek, A. Eisenhauer and M. Dietzel, Sr^{2+}/Ca^{2+} and $^{44}Ca/^{40}Ca$ fractionation during inorganic calcite formation: III. Impact of salinity/ionic strength, *Geochim. Cosmochim. Acta*, 2012, **77**, 432–443.

33 A. R. Taylor, C. Brownlee and G. Wheeler, Coccolithophore Cell Biology: Chalking up progress, *Annu. Rev. Mar. Sci.*, 2017, **9**, 283–310.

34 D. E. Clapham, Calcium signalling, *Cell*, 1995, **80**, 259–268.

35 B. Alberts, A. Johnson, J. Lewis, M. Raff, K. Roberts and P. Walter, *Molecular Biology of the Cell*, Garland Science, New York, 2002.

36 G. Langer, I. Probert, G. Nehrke and P. Ziveri, The morphological response of *Emiliania huxleyi* to seawater carbonate chemistry changes: an inter-strain comparison, *J. Nannoplankton Res.*, 2011, **32**, 29–34.

37 R. B. Lorens, Sr, Cd, Mn, and Co distribution coefficients in calcite as a function of calcite precipitation rate, *Geochim. Cosmochim. Acta*, 1981, **45**, 553–561.

38 A. J. Tosoriero and J. F. Pankow, Solid solution partitioning of Sr^{2+}, Ba^{2+}, and Cd^{2+} to calcite, *Geochim. Cosmochim. Acta*, 1996, **60**, 1053–1063.

39 A. A. Finch and N. Allison, Coordination of Sr and Mg in calcite and aragonite, *Mineral. Mag.*, 2007, **71**, 539–552.

40 J. L. Littlewood, S. Shaw, C. L. Peacock, P. Bots, D. Trivedi and I. T. Burke, Mechanism of Enhanced Strontium Uptake into Calcite via an Amorphous Calcium Carbonate Crystallization Pathway, *Cryst. Growth Des.*, 2017, **17**, 1214–1223.

41 G. Langer, A. Sadekov, G. Nehrke, C. Baggini, R. Rodolfo-Metalpa, J. M. Hall-Spencer, E. Cuoco, J. Bijma and H. Elderfield, Relationship between mineralogy and minor element partitioning in limpets from an Ischia CO2 vent site provides new insights into their biomineralization pathway, *Geochim. Cosmochim. Acta*, 2018, **236**, 218–229.

